GEOPHYSICAL RESEARCH LETTERS, VOL. 35, L16803, doi:10.1029/2008GL034724, 2008

Supercells and mesocyclones in outer rainbands of Hurricane Katrina (2005)

Wen-Chau Lee,[1] Michael M. Bell,[1,2] and Keith E. Goodman Jr.[3]

Received 22 May 2008; revised 8 July 2008; accepted 15 July 2008; published 19 August 2008.

[1] This study documents and describes supercells embedded within the outer rainbands of Hurricane Katrina (2005). Radar reflectivity and velocity data collected on 29 August 2005 by Weather Surveillance Radar 1988 Doppler radars were used to track the supercells. Radar analysis indicates that the supercells were characterized by heavy precipitation collocated with band-relative mesocylonic circulations containing strong vorticity and a wind speed enhancement to their northeast. Atmospheric soundings and dual-Doppler derived shear suggest that environmental conditions were comparable to those in previous hurricane-spawned supercell studies. Twenty-three storms from 0300–0900 UTC were tracked, and single- and dual-Doppler radar analyses were used to examine characteristics such as shear and rotational velocity. Remarkably, the majority of the supercells formed over the Gulf of Mexico rather than over land, which contrasts with previous studies. Furthermore, the ground-relative wind speeds of these potentially tornadic mesocyclones in the outer rainbands could have been Category 4 intensity despite sustained winds in Katrina's eyewall only reaching Category 3 at landfall.
Citation: Lee, W.-C., M. M. Bell, and K. E. Goodman Jr. (2008), Supercells and mesocyclones in outer rainbands of Hurricane Katrina (2005), *Geophys. Res. Lett.*, *35*, L16803, doi:10.1029/2008GL034724.

1. Introduction

[2] Hurricane Katrina (2005) made landfall near Buras-Triumph, Louisiana as a strong Category 3 hurricane at 1110 UTC on 29 August 2005 with a maximum 1-minute sustained surface winds of ~110 kt (~56 m s^{-1}), and a central pressure of 920 hPa (according to the Saffir-Simpson Hurricane Scale, Category 1 is defined as 1-minute sustained surface winds of 64–82 kt. Category 2 is 83–95 kt; Category 3 is 96–113 kt, Category 4 is 114–135 kt; and Category 5 is ≥136 kt). The severe wind and the storm surge of Katrina left catastrophic devastation along the central Gulf Coast states of the U.S. Katrina's unofficial death toll exceeded 1800; the storm was responsible for an estimated $75 billion in damage, making it the costliest in U.S. history [*U.S. Department of Commerce*, 2005]. Hurricane Katrina also spawned documented tornadoes, primarily over the period 29–31 August 2005 from Louisiana to Pennsylvania. Some of the damage from these tornadoes, especially along the Gulf coast, may have been overshadowed by damage caused by strong winds and storm surge from the large primary circulation of the hurricane itself.

[3] It is common for tropical cyclones (TCs) to spawn tornadoes over land [*Novlan and Gray*, 1974; *McCaul*, 1991] in either the "core" region (eyewall or inner rainbands) or outer rainbands (typically 200–400 km from the TC center) [*Gentry*, 1983; *Weiss*, 1987]. Most TC-spawned tornadoes occur in the outer rainbands in the right-front quadrant of TCs on the day of the landfall [e.g., *Smith*, 1965; *Weiss*, 1987]. These tornadoes often occur in areas of high moisture content, low convective available potential energy (~253 J kg^{-1} on average), and strong shear in the low levels [*McCaul*, 1991]. The increase of surface friction in the transition from water to land is commonly attributed to the increasing low-level shear that promotes tornado genesis [*Gentry*, 1983]. These tornadoes are less intense (<F2) than their counterparts in the Great Plains [e.g., *Novlan and Gray*, 1974; *McCaul*, 1987; *McCaul and Weisman*, 1996; *Spratt et al.*, 1997].

[4] Tornadoes over water (waterspouts) associated with landfalling TCs are difficult to identify since waterspouts do not result in damage tracks. The earliest documented TC-spawned waterspout event was associated with the "hook" radar reflectivity signatures in the outer rainbands of Hurricane Carla (1961) [*Rudd*, 1964]. *Dodge et al.* [2000] and *Spratt et al.* [2000] documented strong vertical vorticity ($4–8 \times 10^{-3} s^{-1}$) and CAPE (1200 J kg^{-1}) in a mesocyclone within Hurricane Bonnie's (1998) outer rainbands over water using airborne and coastal Doppler radars and thermodynamic soundings. A nearby cell with similar characteristics moved onshore as a waterspout and produced a documented F1 tornado. More recently, a large waterspout in the outer rainbands of Hurricane Wilma (2005) was photographed near Key West (http://www.srh.noaa.gov/key/HTML/wilma/wilma.html). A Doppler radar cannot observe a tornado or waterspout directly unless it is within several kilometers of the radar, but parent mesocyclones can be detected to identify potential tornadic activity [*Burgess et al.*, 1993]. Statistically, only 26% of Great Plains mesocyclones produce tornadoes [*Trapp et al.*, 2005].

[5] Using reflectivity and Doppler velocity data from Weather Surveillance Radar 1988 Doppler (WSR-88D), *Spratt et al.* [1997] and *McCaul et al.* [2004] examined tornado-producing mesocyclones within outer rainbands of Tropical Storm Gordon (1994), Hurricane Allison (1995) and in the remnants of Tropical Storm Beryl (1994). These tornadic mesocyclones were characterized by 50 dBZ echoes with rotational velocities of 6.5–15 m s^{-1} and core diameters of ~2 km. These parent mesocyclones could last for several hours, be identified ~30 min prior to tornado-

[1]Earth Observing Laboratory, National Center for Atmospheric Research, Boulder, Colorado, USA.
[2]Department of Meteorology, Naval Postgraduate School, Monterey, California, USA.
[3]Department of Physics, Norfolk State University, Norfolk, Virgina, USA.

0094-8276/08/2008GL034724$05.00

genesis, and had an average depth ~3.5 km. Airborne Doppler radar and WSR-88D observations have also indicated that intense mesocyclones can exist in TC eyewall convective bands [e.g., *Stewart and Lyons*, 1996; *Willoughby and Black*, 1996; *Houze et al.*, 2007; *Marks et al.*, 2008].

[6] This paper documents radar signatures of several trains of supercells/mesocyclones in Katrina's outer rainbands before its landfall during a six-hour period. Since these mesocyclones are embedded in background winds of 20–30 m s^{-1}, the local absolute wind speed aloft could be comparable or even stronger than the winds experienced in the eyewall of Katrina. Even higher winds are likely should waterspouts exist within these mesocyclones. As a result, oil rigs and ships that were not in the direct path of Katrina were potentially threatened by these mesocyclones several hundreds of kilometers from Katrina's center, well beyond the path of the eyewall. Results from the Doppler radar analyses of supercells in the outer rainbands are presented in Section 2, followed by a discussion of the results in Section 3.

2. Doppler Radar Analysis

[7] Katrina was observed by two WSR-88D radars located in Slidell, Louisiana, (KLIX), and in Mobile, Alabama (KMOB) before its landfall (Figure 1a). The frequency of radar volume scans is ~5–6 min with a 1° beamwidth and a range resolution of 1 km for reflectivity and 250 m for radial velocity data. The unambiguous range (velocity) was 174 km (21.5 m s^{-1}). Katrina's reflectivity structure can be divided into two regimes; the more coherent inner rainband region (R < 150 km) consisting of eyewall and spiral rainbands, and the outer rainband region (R > 150 km) consisting of more chaotic, cellular convection. While the center of Katrina was still over the Gulf of Mexico at 0604 UTC, the northern part of the outer rainbands had already reached the Gulf Coast. These outer rainbands were composed of individual supercells with mesocyclone Doppler velocity signatures. These supercells moved with the prevailing hurricane circulation within two rainbands at ~200 km and ~250 km from the center. These high radar reflectivity supercells also showed periodic spacing of ~30–40 km along these two rainbands, resembling a train of supercells (Figure 1a).

[8] As noted previously, a tornado circulation can only be observed several kilometers from the radar due to beam broadening with range [*Spratt et al.*, 1997; *McCaul et al.*, 2004; *Lee and Wurman*, 2005]; however, the velocity dipole signature of a parent mesocyclone can be identified at a much longer range from the radar [*Donaldson*, 1970]. When a mesocyclone is embedded in a strong background flow as in a TC rainband, its Doppler velocity signature may appear as strong azimuthal shear rather than a dipole. Radar data (reflectivity and Doppler velocity) at 0.5° elevation angle from 0304 UTC to 0900 UTC were examined.

[9] A detailed look of the radar reflectivity and velocity within the dashed box in Figure 1a is portrayed in Figures 1b and 1c. At least four supercells/mesocyclones (indicated by black circles) are apparent. All Doppler velocities in the study region are negative (i.e., towards the radar), but to illustrate the velocity dipole the Doppler velocity scale in Figures 1a–1c was centered at the background hurricane circulation (~31 m s^{-1}) estimated from the single Doppler radar velocities. Hence, the "cool" ("warm") colors indicate the approaching (receding) flow in rainband-relative sense. These supercells typically possess ~50 dBZ maximum reflectivity, a length scale of ~10–20 km, and a rainband-relative rotational velocity between 20–30 m s^{-1}, similar to their counterparts over land. The diameters of these mesocyclones range from 4–12 km. The mesocyclone #14 possessed a maximum ground-relative Doppler velocity of 61 m s^{-1} at 1–1.5 km altitude (Figure 1c). A moored buoy (42007) (white star in Figure 1b) located near storm #13 stopped reporting at 0600 UTC, the approximate time of mesocylone passage (0604 UTC). The 10-minute averaging time of the buoy winds and uncertainties in reducing Doppler velocities aloft to the surface makes comparing measurements from these platforms difficult, but the coincident failure of the buoy and mesocyclone passage provide some circumstantial evidence for strong winds associated with these features.

[10] Figure 2 presents the tracks of 23 mesocyclones during the six-hour period where their characteristics are summarized in Table 1. Remarkably, most of these tracks, except mesocyclones 1, 21, 22, and 23, were over the Gulf of Mexico. Each storm was numbered chronologically with respect to the approximate time that it dissipated. Note that in contrast to the other storms analyzed, the origins of mesocyclones 17, 19, and 20 were backtracked using reflectivity data because of the 174 km unambiguous velocity range (dashed lines in Figure 2). The lower right corner of Figure 2 shows the bathymetric gradient of the Gulf of Mexico (thin gray contours) with a steep drop off in the ocean depth beyond 100 m near the edge of radar range. The cluster of storms (11, 13, 14, 17, 19, and 20) that originated near this steep gradient approximately 120 km from the Gulf coast generally had longer durations than the other storms originated closer to the coast line. There appears to be a correlation between the bathymetry of the Gulf of Mexico and the development of these supercells over water, but limitations of the Doppler range preclude drawing conclusions from this single dataset.

[11] Documented characteristics of the mesocyclones in Table 1 were the beginning and ending time, maximum diameter (distance between peak dipole velocities), vorticity (twice the difference of the dipole velocities divided by the mesocyclone diameter), and axisymmetric rotational speed (average of the peak dipole velocities). (These maximum properties can occur at different stages of a storm.) The storms tracked in this study were classified as mesocyclones if the vorticity reached 0.01 s^{-1} [*Wicker and Wilhelmson*, 1995] at any point during its lifetime. Next, the storms were classified as tornadic mesocyclones if the maximum rotational speed reached 18 m s^{-1} (F0 intensity) [*Fujita*, 1971]. Eighteen of 23 storms' rotational speed reached F0 intensity aloft at some point during its lifetime. Among these tornadic mesocyclones, storm 11 had the greatest rotational speed at 30.1 m s^{-1}, storm 19 had the greatest ground-relative speed (rotational speed plus the background flow from the hurricane) at 67.2 m s^{-1}, and storm 13 lasted the longest (1 h 50 min). Although the intensities of these tornadic mesocylones were in the high F0 range, the resulting ground-relative circulations were highly asymmetric as illustrated in Figure 1c. The instantaneous ground-relative winds aloft

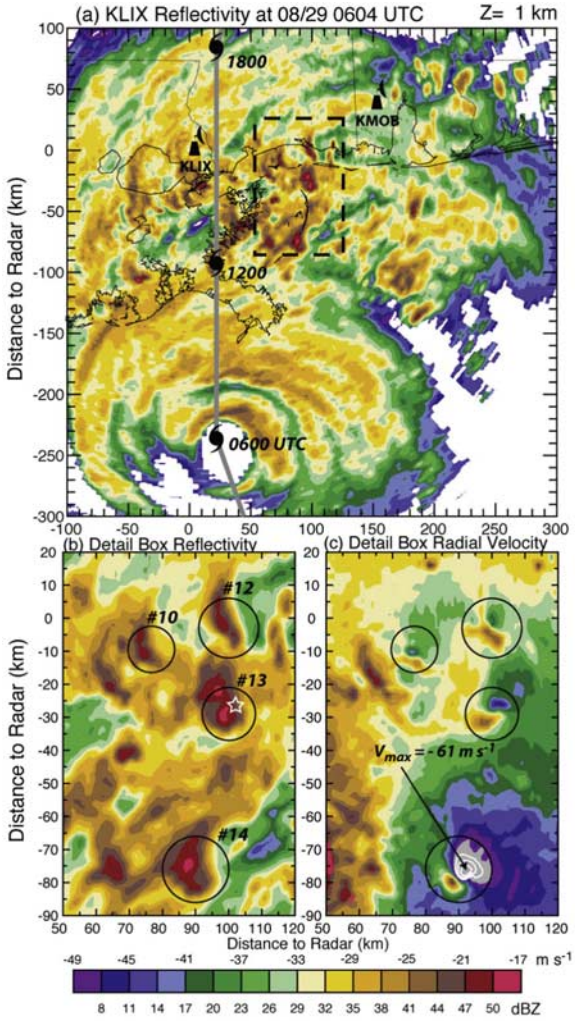

Figure 1. Radar reflectivity and Doppler velocity 1 km CAPPI from KLIX WSR-88D at 0604 UTC 29 August 2005. (a) The 400 × 400 km reflectivity (color, dBZ), radar locations and NHC best track of Hurricane Katrina (hurricane symbols, thick gray line). (b and c) Reflectivity and radial velocity (m s^{-1}) in dashed box indicated in Figure 1a. Mesocyclones 10, 12, 13, and 14 are highlighted with circles. White star in Figure 1b indicates location of buoy 42007. White lines in Figure 1c indicate additional velocity contours beyond −49 m s^{-1}.

reached Category 4 hurricane strength when they were embedded in a background circulation of ∼30 m s^{-1}. A reduction to ∼70–80% of the wind speed obtained at 1 to 1.5 km altitude would be necessary to compare with the hurricane's surface circulation, but it is likely that the maximum winds associated with these mesocyclones were underestimated due to the radar beam spreading with distance, and potential waterspouts embedded within these mesocyclones [*Dodge et al.*, 2000; *Spratt et al.*, 2000]. This suggests that these mesocyclones had the potential for significant damage to oil platforms or other structures in the Gulf several hundreds of kilometers from the Katrina's center.

[12] The location of mesocyclones 12 and 13 (Figure 3a) and 14 (Figure 3b) at 0604 UTC permitted a dual-Doppler analysis from KLIX and KMOB with a baseline ∼150 km in limited-area domains centered on the mesocyclones. The Doppler velocities from KLIX and KMOB were unfolded in radar spherical coordinates using National Center for Atmospheric Research (NCAR) Soloii software, then interpolated onto a common 1.5 km × 1.5 km × 1 km (x, y, z) grid with a horizontal (vertical) radius of influence of 2 km (1.5 km) using Cressman interpolation with NCAR Reorder software, and then synthesized with NCAR CEDRIC software to produce three-dimensional winds [*Cressman*, 1959; *Mohr et al.*, 1986; *Oye et al.*, 1995]. The lowest elevation of the radar beams was 0.5° preventing calculation of winds below 1 km in the analysis domain. The vertical velocity (w) was vertically integrated upward using the continuity equation by assuming $w = 0$ at the sea surface. The background flow were calculated separately for each analysis domain at each level and were subtracted to examine the rainband-relative circulations, shown with vectors in Figures 3a and 3b. The rotation and significant vertical vorticity (gray 1 × 10^{-3}s^{-1} contours) collocated with the reflectivity maxima (color 3 dBZ contours) at 2 km further confirms the mesocylonic structure and similarity to supercellular convection. Probably due to the smoothing in the interpolation and filtering of the synthesized winds, the magnitude of the vorticity at 2 km level is weaker than that derived using the radial velocities at 1 km altitude, but still exceeds 2.5 × 10^{-3}s^{-1} in all three mesocyclones. Wind speed maxima (white 3 m s^{-1} contours) are evident in the NE quadrant of each mesocyclone, where the perturbation winds aligned with the mean flow. The updraft (not shown) correlated with the maximum reflectivity and the maximum vorticity in these mesocyclones, suggesting that positive stretching of vorticity was occurring. In Figure 3c, a clockwise curved hodograph derived from the dual-Doppler mean

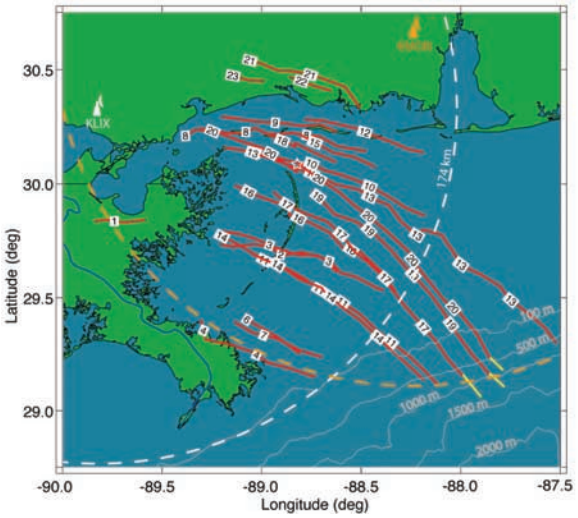

Figure 2. Mesocyclone tracks in Katrina's outer rainbands from 0300–0600 UTC 29 August 2005. Numbers correspond to Table 1. Dashed circles indicate Doppler velocity range of KLIX (white) and KMOB (orange) radars. Thin gray contours denote ocean depths greater than 100 meters. White star indicates location of buoy 42007.

Table 1. Mesocyclone Characteristics Determined by Single Doppler Tracking and Analysis[a]

Storm ID	Begin	End	Max Diameter (km)	Max Vorticity (s^{-1})	Max Rotational Speed (m s^{-1})	Category
1	0304	0326	6.1	0.023	21.5	F0
2	0315	0348	8.2	0.029	29.2	F0
3	0326	0421	8.6	0.025	20.7	F0
4	0343	0415	9.4	0.021	27.5	F0
5	0348	0354	3.5	0.060	25.7	F0
6	0405	0415	6.7	0.012	16.5	<F0
7	0421	0443	7.7	0.011	15.0	NM
8	0410	0521	6.7	0.035	22.5	F0
9	0454	0532	5.9	0.037	21.7	F0
10	0505	0559	8.8	0.032	24.5	F0
11*	0441	0553	9.4	0.046	30.1	F0
12	0526	0605	7.9	0.028	18.0	<F0
13	0436	0627	8.2	0.019	19.7	F0
14*	0519	0621	11.2	0.018	25.5	F0
15	0638	0659	4.8	0.039	20.2	F0
16	0624	0716	8.7	0.025	25.0	F0
17*	0608	0716	8.0	0.030	26.7	F0
18	0732	0754	5.8	0.048	14.0	<F0
19*	0713	0810	10.1	0.041	18.1	F0
20	0729	0900	8.2	0.023	25.7	F0
21	0821	0859	10.7	0.011	13.5	F0
22	0821	0832	8.2	0.005	6.0	NM
23	0832	0843	5.1	0.012	13.0	F0

[a]All times are UTC on 29 Aug 2005. Storms marked with an asterisk (*) started at a time before entering the Doppler range, therefore prior mesocyclone characteristics could not be estimated. In the final column, F0 (F scale) = Mesocyclones' winds were between 18–32 m/sec; <F0 = Mesocyclones' winds never reached F0 intensity; NM = Not a mesocyclone.

wind in Figure 3a shows that the low-level (1–6 km) shear vector is ~23 m s^{-1} from the SSW (200°), with a ~35 m s^{-1} mean wind vector to the left of this by ~70 degrees. A radiosonde launched from Slidell at 0000 UTC outside of the rainbands had ~1000 J kg^{-1} of CAPE. Using these values, a Bulk Richardson Number (BRN) defined as the ratio of low-level environmental wind shear and thermodynamic stability is estimated at 3.2, indicating the local environment appears to be favorable for supercell development [*Weisman and Klemp*, 1984].

3. Summary and Discussion

[13] Previous studies in the formation of TC-induced tornadoes have been focused on tornadoes that occurred over land where the low-level horizontal vorticity can be drastically enhanced by the increasing roughness of the land surface compared to the water. This paper uses Doppler radar data to document the low-level structures of trains of supercells/mesocyclones embedded in Katrina's outer rainbands over the Gulf of Mexico as the TC approached the Gulf coast. The likelihood of having TC-induced waterspouts over the ocean 200 km away from Katrina's center posed a potential threat to numerous oil platforms near the Gulf Coast and coastal residences even they were not directly hit by Katrina's eyewall. The features reported in this study may be more common than an isolated event in Hurricane Katrina; the authors are aware of similar over-water supercells/mesocyclones embedded in the outer rainbands of Hurricanes Bonnie (1998), Lenny (1999), and Ivan (2004).

[14] Observations from Doppler radar and rawindsondes suggest that strong low-level shear did exist and the BRN of ~3.2 was a favorable environment for supercell formation. We speculate that a modification of the sea state over the continental shelf [*Walsh et al.*, 2002] might have increased the low-level shear and/or decreased the low-level stability, creating a more favorable BRN for supercell development. Another possible factor may have been interaction with a continental air mass prior to landfall, although no obvious dry air around the rainbands was evident in satellite imagery (not shown). Other mechanisms are possible, and further speculation from this limited dataset is not justified. Addi-

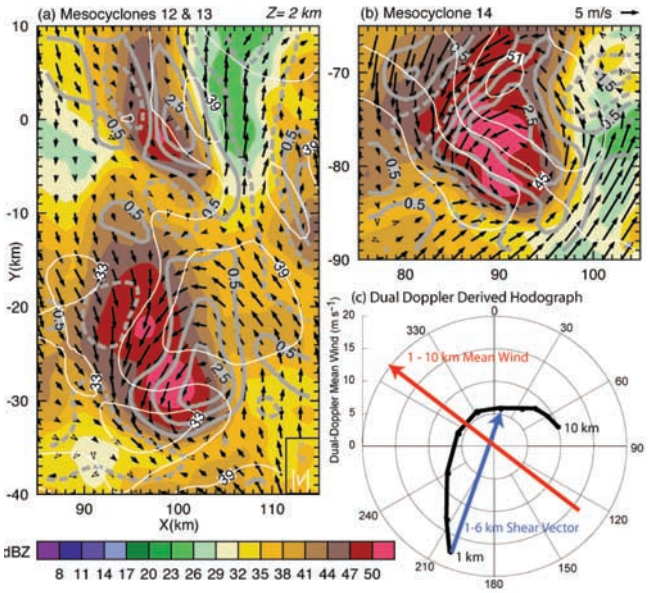

Figure 3. Dual-Doppler analysis at 2 km of mesocyclones (a) 12, 13, and (b) 14 from KLIX and KMOB radars. Reflectivity (color, dBZ) is overlaid with rainband-relative wind vectors, relative vertical vorticity ($1 \times 10^{-3} s^{-1}$ gray contours), and wind speed magnitude (3 m s^{-1} white contours). (c) Hodograph derived from area-averaged wind in domain of Figure 3a, volume averaged mean wind vector (red), and 1–6 km shear vector (blue).

tional observations and numerical modeling studies are needed to develop more extensive documentation of TC-spawned mesocyclones and explore different mechanisms for supercell generation over water.

[15] **Acknowledgments.** Reviews provided by Roger Wakimoto, Chris Davis, Scott Ellis and two anonymous reviewers greatly improved this manuscript. We would also like to acknowledge the NCAR SOARS program for funding the summer visit of the third author to begin this research, and the National Weather Service and National Climactic Data Center for collecting and archiving the NEXRAD Level II data used in this study. The National Center for Atmospheric Research is sponsored by the National Science Foundation.

References

Burgess, D. W., R. J. Donaldson Jr., and P. R. Desrochers (1993), Tornado detection and warning by radar, in *The Tornado: Its Structure, Dynamics, Prediction, and Hazards, Geophys. Monogr. Ser.*, vol. 79, edited by C. Church et al., pp. 203–221, AGU, Washington, D. C.

Cressman, G. P. (1959), An operational objective analysis system, *Mon. Weather Rev.*, *87*, 367–374.

Dodge, P., S. Spratt, F. D. Marks Jr., D. Sharp, and J. Gamache (2000), Dual-Doppler analyses of mesovortices in a hurricane rainband, paper presented at 24th Conference on Hurricanes and Tropical Meteorology, Am. Meteorol. Soc., Fort Lauderdale, Fla.

Donaldson, R. J., Jr. (1970), Vortex signature recognition by a Doppler radar, *J. Appl. Meteorol.*, *9*, 661–670.

Fujita, T. (1971), Proposed characterization of tornadoes and hurricanes by area and intensity, *SMRP Res. Pap. 91*, 42 pp., Univ. of Chicago, Chicago, Ill.

Gentry, R. C. (1983), Genesis of tornadoes associated with hurricanes, *Mon. Weather Rev.*, *111*, 1793–1805.

Houze, R. A., Jr., S. S. Chen, B. F. Smull, W.-C. Lee, and M. M. Bell (2007), Hurricane intensity change and eyewall replacement, *Science*, *315*, 1235–1239.

Lee, W.-C., and J. Wurman (2005), Diagnosed three-dimensional axisymmetric structure of the Mulhall Tornado on 3 May 1999, *J. Atmos. Sci.*, *62*, 2373–2393.

Marks, F. D., P. G. Black, M. T. Montgomery, and R. W. Burpee (2008), Structure of the eye and eyewall of Hurricane Hugo, 1989, *Mon. Weather Rev.*, *136*, 1237–1259.

McCaul, E. W., Jr. (1987), Observations of the Hurricane "Danny" tornado outbreak of 16 August 1985, *Mon. Weather Rev.*, *115*, 1206–1223.

McCaul, E. W., Jr. (1991), Buoyancy and shear characteristics of hurricane-tornado environments, *Mon. Weather Rev.*, *119*, 1954–1978.

McCaul, E. W., and M. L. Weisman (1996), Simulations of shallow supercell storms in landfalling hurricane environments, *Mon. Weather Rev.*, *134*, 408–429.

McCaul, E. W., D. E. Buechler, S. J. Goodman, and M. Cammarata (2004), Doppler radar and lightning network observation of a severe outbreak of tropical cyclone tornadoes, *Mon. Weather Rev.*, *132*, 1747–1763.

Mohr, C. G., L. Jay Miller, R. L. Vaughan, and H. W. Frank (1986), The merger of mesoscale datasets into a common Cartesian format for efficient and systematic analyses, *J. Atmos. Oceanic Technol.*, *3*, 143–161.

Novlan, D. J., and W. M. Gray (1974), Hurricane spawned tornadoes, *Mon. Weather Rev.*, *102*, 476–488.

Oye, R., C. Mueller, and S. Smith (1995), Software for radar translation, visualization, editing, and interpolation, paper presented at 27th Conference on Radar Meteorology, Am. Meteorol. Soc., Vail, Colo.

Rudd, M. I. (1964), Tornadoes during Hurricane Carla at Galveston, *Mon. Weather Rev.*, *92*, 251–254.

Smith, J. S. (1965), The hurricane-tornado, *Mon. Weather Rev.*, *93*, 453–459.

Spratt, S. M., D. W. Sharp, P. Welsh, A. Sandrik, F. Alsheimer, and C. Paxton (1997), A WSR-88D assessment of tropical cyclone outer rainband tornadoes, *Weather Forecast.*, *12*, 479–501.

Spratt, S. M., F. D. Marks Jr., and P. Dodge (2000), Examining the pre landfall environment of hurricane outer rainband mesovortices, paper presented at 24th Conference on Hurricanes and Tropical Meteorology, Am. Meteorol. Soc., Fort Lauderdale, Fla.

Stewart, S. R., and S. W. Lyons (1996), A WSR-88D radar view of tropical cyclone Ed, *Weather Forecast.*, *11*, 115–135.

Trapp, R. J., G. J. Stumpf, and K. L. Manross (2005), A reassessment of the percentage of tornadic mesocyclones, *Weather Forecast.*, *20*, 680–687.

U.S. Department of Commerce (2005), Service assessment of Hurricane Katrina August 23–31, 2005, NOAA, Silver Spring, Md.

Walsh, E. J., C. W. Wright, D. Vandemark, W. B. Krabill, A. W. Garcia, S. H. Houston, S. T. Murillo, M. D. Powell, P. G. Black, and F. D. Marks (2002), Hurricane directional wave spectrum spatial variation at landfall, *J. Phys. Oceanogr.*, *32*, 1667–1684.

Weisman, M. L., and J. B. Klemp (1984), The structure and classification of numerically simulated convective storms in directionally varying wind shears, *Mon. Weather Rev.*, *112*, 2479–2498.

Weiss, S. J. (1987), Some climatological aspects of forecasting tornadoes associated with tropical cyclones, paper presented at 17th Conference on Hurricanes and Tropical Meteorology, Am. Meteorol. Soc., Miami, Fla.

Wicker, L. J., and R. B. Wilhelmson (1995), Simulation and analysis of tornado development and decay within a three-dimensional supercell thunderstorm, *J. Atmos. Sci.*, *52*, 2675–2703.

Willoughby, H. E., and P. G. Black (1996), Hurricane Andrew in Florida: Dynamics of a disaster, *Bull. Am. Meteorol. Soc.*, *77*, 543–549.

M. M. Bell and W.-C. Lee, Earth Observing Laboratory, National Center for Atmospheric Research, P.O. Box 3000, Boulder, CO 80307, USA. (wenchau@ucar.edu)

K. E. Goodman Jr., Department of Physics, Norfolk State University, Norfolk, VA 23504, USA.